A flexible cross-talk simulator for multiple spatial-mode free-space optical communication

Invited Paper

A Flexible Cross-Talk Simulator for Multiple Spatial-Mode Free-Space Optical Communication

Jeffrey H. Shapiro

Massachusetts Institute of Technology, Research Laboratory of Electronics,
Cambridge, MA 02139-4307, USA

ABSTRACT

Laser communication with both high photon information efficiency (many bits/detected-photon) and high spectral efficiency (many bits/sec-Hz) is impossible with a single spatial-mode free-space link. Achieving these high efficiencies in the same system requires operation with 10's to 1000's of high-transmissivity spatial modes. Such systems will likely be restricted to 1 to 10 km line-of-sight terrestrial paths on which turbulence-induced cross talk will be encountered. In this paper we propose a cross-talk simulator for multiple spatial-mode free-space optical communication that could provide valuable information about the relevant merits of different mode sets when they are employed in conjunction with real modal multiplexers and demultiplexers.

Keywords: free-space optical communication, multiple spatial-mode communication, atmospheric turbulence, cross talk

1. INTRODUCTION

Achieving high photon information efficiency (many bits/detected-photon) and high spectral efficiency (many bits/sec-Hz) is impossible with a single spatial-mode free-space communication link [1]. This is so even though high photon information efficiency (PIE) can be obtained with pulse-position modulation (PPM) and direct detection [2], and high spectral efficiency (SE) can be achieved with quadrature amplitude modulation and coherent detection [3]. In particular, PPM's high PIE comes at the cost of low SE, and the PIE of coherent detection systems cannot exceed 3 bits/detected-photon. Achieving high PIE and high SE in the same vacuum-propagation system is possible, but it requires operation with 10's to 1000's of high-transmissivity spatial modes [1]. Consequently, such systems will likely be restricted to 1 to 10 km line-of-sight paths to avoid the need for inordinately large optics. Accordingly, terrestrial applications, with the concomitant atmospheric turbulence must be accounted for.

Recent theoretical work has established ultimate limits on the PIE/SE behavior of multiple spatial-mode free-space communications when the turbulence is uniformly distributed along the propagation path [4,5]. These studies have considered operation both with and without adaptive optics, and explored three possible spatial-mode sets: focused-beam modes, Hermite-Gaussian modes, and Laguerre-Gaussian modes. Table-top experiments, using orbital angular momentum modes—specifically the Laguerre-Gaussian modes with lowest-order radial dependence—have measured cross talk and communication performance with and without adaptive optics for simulated thin (phase-screen) turbulence [6, 7].

In this paper we propose a simple and flexible cross-talk simulator for multiple spatial-mode free-space optical communication. Whereas the theory from [4,5] would be exceedingly tedious to repeat for arbitrary distributions of turbulence along the propagation path, and the experiments from [6,7] have been limited to one mode set and thin turbulence, our proposed simulator can realize arbitrary path distributions for the turbulence, and it can be used with arbitrary mode sets. Moreover, it can be readily implemented. All that is needed are two spatial light modulators: one for the transmitter's exit pupil and one for the receiver's entrance pupil. There are some limitations to this approach: it only simulates an approximation to Kolmogorov-spectrum turbulence, and it only provides information about the average modal cross talk without the use of adaptive optics. Nevertheless, it could provide valuable information about the relevant merits of different mode sets when they are employed in conjunction with real modal multiplexers and demultiplexers.

Send correspondence to jhs@mit.edu.

Laser Communication and Propagation through the Atmosphere and Oceans III, edited by Alexander M. J. van Eijk, Christopher C. Davis, Stephen M. Hammel, Proc. of SPIE Vol. 9224, 922408 © 2014 SPIE
CCC code: 0277-786X/14/$18 · doi: 10.1117/12.2063520

The remainder of this paper is organized as follows. In Section 2, we introduce the propagation geometry for multiple spatial-mode free-space optical communication and reprise results from [4] for evaluating the average modal cross-talk behavior encountered on such a link. Then, in Section 3, we review the use of the extended Huygens-Fresnel principle's Green's-function mutual coherence [8] to perform that evaluation for Kolmogorov-spectrum turbulence. There we also introduce and discuss the square-law approximation to the 5/3-law two-source, spherical-wave wave structure function of Kolmogorov-spectrum turbulence. Reference 4 used that square-law approximation to evaluate the average cross-talk behavior of focused-beam, Hermite-Gaussian, and Laguerre-Gaussian modes when the turbulence was uniformly distributed along the propagation path. That evaluation, however, entailed considerable computational difficulties, even with the simplification afforded by the assumption of square transmitter and receiver pupils equipped, respectively, with ideal modal multiplexers and demultiplexers. The heart of this paper is Section 4, where we show how a simple arrangement with two spatial light modulators (SLMs)—one in the transmitter pupil and one in the receiver pupil—can be used as a physical simulator for an arbitrary path distribution of turbulence. This simulator determines the average modal cross-talk behavior via the square-law approximation to the two-source, spherical-wave wave structure function of Kolmogorov-spectrum turbulence. Moreover, because it is a physical simulator, it can assess the average cross talks encountered with any desired pupil geometries and mode sets when real modal multiplexers and demultiplexers are employed.

2. MULTIPLE SPATIAL-MODE FREE-SPACE OPTICAL COMMUNICATION

Consider a line-of-sight atmospheric propagation path between a transmitter exit pupil $\mathcal{A}_T$ in the $z = 0$ plane and a receiver entrance pupil $\mathcal{A}_R$ in the $z = L$ plane. These will be taken to be coaxial and circular, i.e., $\mathcal{A}_T = \{\boldsymbol{\rho} = (x, y) : |\boldsymbol{\rho}| \leq D_T/2\}$ and $\mathcal{A}_R = \{\boldsymbol{\rho}' = (x', y') : |\boldsymbol{\rho}'| \leq D_R/2\}$, as shown in Fig. 1, although other configurations could easily be accommodated in what follows. We will assume that a linearly-polarized laser transmission—center wavelength λ, scalar complex-field envelope $E_T(\boldsymbol{\rho}, t)$ with $\sqrt{\text{W}}/\text{m}$ units—is sent from $\mathcal{A}_T$, resulting in reception of a linearly-polarized field with scalar complex envelope $E_R(\boldsymbol{\rho}', t)$, again with $\sqrt{\text{W}}/\text{m}$ units, in $\mathcal{A}_R$.*

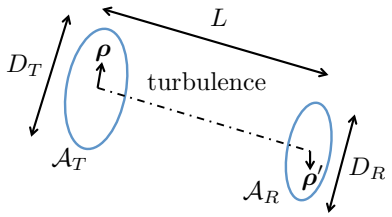

Figure 1: Atmospheric-path propagation geometry.

From the extended Huygens-Fresnel principle [8], we have that $E_R(\boldsymbol{\rho}', t)$ is related to $E_T(\boldsymbol{\rho}, t)$, by the superposition integral

$$E_R(\boldsymbol{\rho}', t) = \int_{\mathcal{A}_T} d\boldsymbol{\rho}\, E_T(\boldsymbol{\rho}, t - L/c) h(\boldsymbol{\rho}', \boldsymbol{\rho}, t), \text{ for } \boldsymbol{\rho}' \in \mathcal{A}_R, \tag{1}$$

where $h(\boldsymbol{\rho}', \boldsymbol{\rho}, t)$ is the atmospheric Green's function at time t, and we have exploited the fact that turbulence-induced multipath spread is sub-ps and that Gbps communication can be accomplished with ns-duration pulses in assuming that the temporal behavior is just the line-of-sight propagation delay L/c. Furthermore, because the coherence time of the turbulence is ∼ms, we can safely limit our attention to a single atmospheric state and suppress the Green's function's time argument.

For multiple spatial-mode free-space optical communication we rely on the near-field power transfer characteristic of the Fig. 1 propagation geometry that exists when its free-space Fresnel-number product, $D_f \equiv$

*No loss of generality is incurred by employing a scalar-wave theory, because turbulence does not cause depolarization [9].

$(\pi D_T D_R/4\lambda L)^2$ is much greater than 1 [10]. To understand why this is so, we introduce the atmospheric Green's function's singular-value decomposition,

$$h(\boldsymbol{\rho}', \boldsymbol{\rho}) = \sum_{m=1}^{\infty} \sqrt{\eta_m}\, \psi_m(\boldsymbol{\rho}') \Psi_m^*(\boldsymbol{\rho}), \text{ for } \boldsymbol{\rho} \in \mathcal{A}_T \text{ and } \boldsymbol{\rho}' \in \mathcal{A}_R, \tag{2}$$

where: $\{\, \Psi_m(\boldsymbol{\rho}) : 1 \le m < \infty, \boldsymbol{\rho} \in \mathcal{A}_T \,\}$ is a complete orthonormal (CON) set of input modes on $\mathcal{A}_T$; $\{\, \psi_m(\boldsymbol{\rho}') : 1 \le m < \infty, \boldsymbol{\rho}' \in \mathcal{A}_R \,\}$ is a CON set of output modes on $\mathcal{A}_R$; $\{\, \eta_m : 1 \le m < \infty \,\}$ is their associated power-transfer eigenvalues; and the modes have been ordered such that $1 \ge \eta_1 \ge \eta_2 \ge \cdots \ge \eta_m \ge \cdots 0$. Physically, Eq. (2) implies that transmission of $\Psi_m(\boldsymbol{\rho})$ from $\mathcal{A}_T$ results in reception of $\sqrt{\eta_m}\, \psi_m(\boldsymbol{\rho}')$ in $\mathcal{A}_R$, indicating that η_m is the fractional power transfer from $\mathcal{A}_T$ to $\mathcal{A}_R$ accomplished by this transmission. Moreover, when $D_f \gg 1$, there are approximately D_f input modes with near-unity power-transfer eigenvalues, while those for the remaining modes are all near zero.

Unfortunately, the turbulent atmosphere's input modes, output modes, and power-transfer eigenvalues are all, in general, stochastic. Thus, unless adaptive optics is employed at the transmitter and/or the receiver, an M-ary spatial-mode system will multiplex some fixed set of orthonormal spatial modes, $\{\, \Psi_m^{(0)}(\boldsymbol{\rho}) : 1 \le m \le M, \boldsymbol{\rho} \in \mathcal{A}_T \,\}$, into its transmitted field

$$E_T(\boldsymbol{\rho}, t) = \sum_{m=1}^{M} E_{T_m}(t) \Psi_m^{(0)}(\boldsymbol{\rho}), \tag{3}$$

where $\{E_{T_m}(t) : 1 \le m \le M\}$ is a set of information-bearing time signals, and demultiplex the received field using another another fixed M-ary orthonormal mode set, $\{\psi_m^{(0)}(\boldsymbol{\rho}', t) : 1 \le m \le M\}$, to obtain[†]

$$E_{R_m}(t) = \sum_{m=1}^{M} \int_{\mathcal{A}_R} d\boldsymbol{\rho}'\, \psi_m^{(0)*}(\boldsymbol{\rho}') E_R(\boldsymbol{\rho}', t). \tag{4}$$

The normal-mode decomposition for vacuum propagation between coaxial circular pupils is deterministic and known [12], so it provides a possible choice for the $\{\Psi_m^{(0)}(\boldsymbol{\rho})\}$ and the $\{\psi_m^{(0)}(\boldsymbol{\rho}')\}$. Indeed taking $\{\, \Psi_m^{(0)}(\boldsymbol{\rho}) : 1 \le m \le M, \boldsymbol{\rho} \in \mathcal{A}_T \,\}$ and $\{\psi_m^{(0)}(\boldsymbol{\rho}', t) : 1 \le m \le M\}$ to be vacuum propagation's input and output modes with the highest associated power-transfer eigenvalues, $\{\eta_m^{(0)} : 1 \le m \le M\}$, we find that in the absence of turbulence there is no cross talk between the M spatial modes,

$$E_{R_m}(t) = \sqrt{\eta_m^{(0)}}\, E_{T_m}(t - L/c), \text{ for } 1 \le m \le M. \tag{5}$$

In practice, more easily implementable choices are typically considered, including focused-beam (FB) modes, Hermite-Gaussian (HG) modes, and Laguerre-Gaussian (LG) modes [4]. The LG modes have received considerable interest because they carry orbital angular momentum (OAM) [6,7]. Theory has shown, however, that they are unitarily equivalent to the HG modes [4], hence any free-space optical communication advantage they might enjoy over HG modes would be one of implementation simplicity rather than one of a fundamental nature [5]. Our principal concern is evaluating the average cross talk that does occur when we use fixed sets of input and output modes and turbulence is present in the propagation path.

To make explicit the intermodal cross talk that is implicit in Eq. (4) when propagation is through atmospheric turbulence, we use the extended Huygens-Fresnel principle in conjunction with Eq. (3) to rewrite $E_{R_m}(t)$ as

$$E_{R_{m'}}(t) = \sum_{m=1}^{M} E_{T_m}(t - L/c) \int_{\mathcal{A}_R} d\boldsymbol{\rho}' \int_{\mathcal{A}_T} d\boldsymbol{\rho}\, \psi_{m'}^{(0)*}(\boldsymbol{\rho}') h(\boldsymbol{\rho}', \boldsymbol{\rho}) \Psi_m^{(0)}(\boldsymbol{\rho}), \tag{6}$$

so that

$$C_{m,m'} \equiv \left\langle \left| \int_{\mathcal{A}_R} d\boldsymbol{\rho}' \int_{\mathcal{A}_T} d\boldsymbol{\rho}\, \psi_{m'}^{(0)*}(\boldsymbol{\rho}') h(\boldsymbol{\rho}', \boldsymbol{\rho}) \Psi_m^{(0)}(\boldsymbol{\rho}) \right|^2 \right\rangle \tag{7}$$

for $m \ne m'$ gives the unnormalized average cross talk between modes m and m'.

[†]A general procedure for optical extraction of multiple spatial modes is given in [11].

3. EVALUATING AVERAGE INTERMODAL CROSS TALK

Evaluation of the average intermodal cross talk incurred in the Fig. 1 setup can be done from knowledge of the atmospheric Green's function's mutual coherence function, $\langle h^*(\boldsymbol{\rho}_1'\boldsymbol{\rho}_1)h(\boldsymbol{\rho}_2',\boldsymbol{\rho}_2)\rangle$, because Eq. (7) can be expanded to yield

$$C_{m,m'} = \int_{\mathcal{A}_R} d\boldsymbol{\rho}_1' \int_{\mathcal{A}_R} d\boldsymbol{\rho}_2' \int_{\mathcal{A}_T} d\boldsymbol{\rho}_1 \int_{\mathcal{A}_T} d\boldsymbol{\rho}_2\, \psi_{m'}^{(0)}(\boldsymbol{\rho}_1')\psi_{m'}^{(0)*}(\boldsymbol{\rho}_2')\Psi_m^{(0)*}(\boldsymbol{\rho}_1)\Psi_m^{(0)}(\boldsymbol{\rho}_2)\langle h^*(\boldsymbol{\rho}_1',\boldsymbol{\rho}_1)h(\boldsymbol{\rho}_2',\boldsymbol{\rho}_2)\rangle. \tag{8}$$

For Kolmogorov-spectrum turbulence, we have that [8,13,14]

$$\langle h^*(\boldsymbol{\rho}_1',\boldsymbol{\rho}_1)h(\boldsymbol{\rho}_2',\boldsymbol{\rho}_2)\rangle = \frac{e^{-ik(|\boldsymbol{\rho}_1'-\boldsymbol{\rho}_1|^2-|\boldsymbol{\rho}_2'-\boldsymbol{\rho}_2|^2)/2L}}{(\lambda L)^2}\, e^{-D(\boldsymbol{\rho}_1'-\boldsymbol{\rho}_2',\boldsymbol{\rho}_1-\boldsymbol{\rho}_2)/2}, \tag{9}$$

where $k = 2\pi/\lambda$ is the wave number, the fraction on the right is due to vacuum propagation, and

$$D(\boldsymbol{\rho}_1'-\boldsymbol{\rho}_2',\boldsymbol{\rho}_1-\boldsymbol{\rho}_2) \equiv 2.91k^2 \int_0^L dz\, C_n^2(z)|(\boldsymbol{\rho}_1'-\boldsymbol{\rho}_2')z/L + (\boldsymbol{\rho}_1-\boldsymbol{\rho}_2)(1-z/L)|^{5/3}, \tag{10}$$

is due to turbulence, whose strength profile along the path is $C_n^2(z)$. The initial derivation of this mutual coherence function employed the Rytov approximation [8,13], hence $D(\boldsymbol{\rho}_1'-\boldsymbol{\rho}_2',\boldsymbol{\rho}_1-\boldsymbol{\rho}_2)$ was termed the two-source, spherical-wave wave structure function, and the validity of Eqs. (9) and (10) was limited to the weak-perturbation regime before the onset of saturated scintillation. Later [14], it was shown that Eqs. (9) and (10) could be obtained from the parabolic equation without the Rytov approximation, making them valid well into saturated scintillation.

Exact evaluation of $\{C_{m,m'} : 1 \le m, m' \le M\}$ from Eqs. (8)–(10) for an arbitrary $C_n^2(z)$ profile and $M \gg 1$ is computationally prohibitive. Each $C_{m,m'}$ evaluation requires an eight-dimensional numerical integration whose integrand requires its own numerical evaluation, because there is no closed-form expression for $D(\boldsymbol{\rho}_1'-\boldsymbol{\rho}_2',\boldsymbol{\rho}_1-\boldsymbol{\rho}_2)$ even when the turbulence is uniformly distributed. That is why our prior numerical evaluation [4] of $C_{m,m'}$ exploited the rectangular symmetry of the FB and HG modes when $\mathcal{A}_T$ and $\mathcal{A}_R$ are $d\times d$ square pupils, together with the square-law approximation to Eq. (10) for uniformly-distributed turbulence, so that four-dimensional integrations over closed-form integrands were sufficient for 225 FB modes and 231 HG modes. Then, by means of the unitary relationship between sets of HG and LG modes, we obtained $C_{m,m'}$ values for 231 modes of the latter set from the calculated cross talks for the corresponding 231 modes of the former set. The present paper's goal is more ambitious. By making the square-law approximation to Eq. (10) that applies for non-uniform turbulence distributions, we seek a flexible physical simulator capable of measuring $C_{m,m'}$ values for arbitrary pupil shapes, mode sets, and turbulence distributions. Thus we will complete this section by developing and discussing the square-law approximation, postponing description of the simulator until Section 4.

The square-law approximation to Eq. (10) that we shall employ is [15]

$$D(\boldsymbol{\rho}_1'-\boldsymbol{\rho}_2',\boldsymbol{\rho}_1-\boldsymbol{\rho}_2) = \frac{|\boldsymbol{\rho}_1'-\boldsymbol{\rho}_2'|^2W' + (\boldsymbol{\rho}_1'-\boldsymbol{\rho}_2')\cdot(\boldsymbol{\rho}_1-\boldsymbol{\rho}_2)(8/3-W'-W) + |\boldsymbol{\rho}_1-\boldsymbol{\rho}_2|^2W}{\rho_u^2}, \tag{11}$$

where W' and W are path-weighting terms, given by

$$W' = \frac{8\displaystyle\int_0^L dz\,(z/L)^2C_n^2(z)}{3\displaystyle\int_0^L dz\,C_n^2(z)} \quad \text{and} \quad W = \frac{8\displaystyle\int_0^L dz\,(1-z/L)^2C_n^2(z)}{3\displaystyle\int_0^L dz\,C_n^2(z)} \tag{12}$$

and ρ_u is the spherical-wave turbulence coherence length for a uniform turbulence distribution with the same integrated strength as the actual distribution,

$$\rho_u = \left(1.09k^2\int_0^L dz\,C_n^2(z)\right)^{-3/5}. \tag{13}$$

For a uniform turbulence distribution, this approximation reduces to

$$D(\boldsymbol{\rho}_1' - \boldsymbol{\rho}_2', \boldsymbol{\rho}_1 - \boldsymbol{\rho}_2) = \frac{8(|\boldsymbol{\rho}_1' - \boldsymbol{\rho}_2'|^2 + (\boldsymbol{\rho}_1' - \boldsymbol{\rho}_2')\cdot(\boldsymbol{\rho}_1 - \boldsymbol{\rho}_2) + |\boldsymbol{\rho}_1 - \boldsymbol{\rho}_2|^2)}{9\rho_0^2}, \tag{14}$$

where $\rho_0 = (1.09k^2C_n^2L)^{-3/5}$, which equals 8/9 times what we used in [4].

There is a crucial point to be made at this juncture. The early work on the extended Huygens-Fresnel principle was based on the Rytov approximation [8], hence it expressed the atmospheric Green's function as

$$h(\boldsymbol{\rho}', \boldsymbol{\rho}) = \frac{e^{ik(L+|\boldsymbol{\rho}'-\boldsymbol{\rho}|^2/2L)}}{i\lambda L}\, e^{\chi(\boldsymbol{\rho}', \boldsymbol{\rho}) + i\phi(\boldsymbol{\rho}', \boldsymbol{\rho})}, \tag{15}$$

i.e., as the vacuum-propagation Fresnel-diffraction Green's function multiplied by the logamplitude and phase fluctuations—$\chi(\boldsymbol{\rho}', \boldsymbol{\rho})$ and $\phi(\boldsymbol{\rho}', \boldsymbol{\rho})$, respectively—that turbulence imposes on the field received at $\boldsymbol{\rho}'$ in the $z = L$ plane from a point source located at $\boldsymbol{\rho}$ in the $z = 0$ plane. Moreover, under the Rytov approximation, $\chi(\boldsymbol{\rho}', \boldsymbol{\rho})$ and $\phi(\boldsymbol{\rho}', \boldsymbol{\rho})$ are jointly-Gaussian random processes. A consequence of their jointly-Gaussian distribution is that

$$D(\boldsymbol{\rho}_1' - \boldsymbol{\rho}_2', \boldsymbol{\rho}_1 - \boldsymbol{\rho}_2) = \langle[\chi(\boldsymbol{\rho}_1', \boldsymbol{\rho}_1) - \chi(\boldsymbol{\rho}_2', \boldsymbol{\rho}_2)]^2\rangle + \langle[\phi(\boldsymbol{\rho}_1', \boldsymbol{\rho}_1) - \phi(\boldsymbol{\rho}_2', \boldsymbol{\rho}_2)]^2\rangle. \tag{16}$$

Wandzura [16] showed that combining the jointly-Gaussian condition with the square-law approximation for this two-source, spherical-wave wave structure function implies that

$$\chi(\boldsymbol{\rho}', \boldsymbol{\rho}) + i\phi(\boldsymbol{\rho}', \boldsymbol{\rho}) = i[\phi_0 + \boldsymbol{\rho}\cdot\nabla\phi_0 + \boldsymbol{\rho}'\cdot\nabla\phi_L], \tag{17}$$

where

$$\phi_0 \equiv \phi(\mathbf{0}, \mathbf{0}), \quad \nabla\phi_0 \equiv \nabla_{\boldsymbol{\rho}}\phi(\boldsymbol{\rho}', \boldsymbol{\rho})|_{\boldsymbol{\rho}=\mathbf{0}, \boldsymbol{\rho}'=\mathbf{0}}, \quad \nabla\phi_L \equiv \nabla_{\boldsymbol{\rho}'}\phi(\boldsymbol{\rho}', \boldsymbol{\rho})|_{\boldsymbol{\rho}=\mathbf{0}, \boldsymbol{\rho}'=\mathbf{0}} \tag{18}$$

are jointly-Gaussian distributed. In simple physical terms, the Rytov approximation plus the square-law approximation to $D(\boldsymbol{\rho}_1' - \boldsymbol{\rho}_2', \boldsymbol{\rho}_1 - \boldsymbol{\rho}_2)$ requires that the turbulence-induced fluctuations in the atmospheric Green's function consist solely of a piston phase, a phase tilt in $z = 0$, and a phase tilt in $z = L$.

A jointly-Gaussian distribution for $\chi(\boldsymbol{\rho}', \boldsymbol{\rho})$ and $\phi(\boldsymbol{\rho}', \boldsymbol{\rho})$ is completely characterized by these fluctuations' first and second moments. Hence the fourth-order moment of $h(\boldsymbol{\rho}', \boldsymbol{\rho})$—needed to quantify beam-wave scintillation behavior—can be found from first and second-moment knowledge. Reference 16 thus invalidates that approach to quantifying beam-wave scintillation when the square-law approximation for the Green's function's mutual coherence function is made. Note that this issue does *not* impact our previous cross-talk analyses [4, 5]. These papers only make use of the Green's function's mutual coherence function. They neither assume that $\chi(\boldsymbol{\rho}', \boldsymbol{\rho})$ and $\phi(\boldsymbol{\rho}', \boldsymbol{\rho})$ are jointly Gaussian, nor use such an assumption to derive a higher-order Green's function moment.

The piston-plus-tilt nature of jointly-Gaussian $\chi(\boldsymbol{\rho}', \boldsymbol{\rho})$ and $\phi(\boldsymbol{\rho}', \boldsymbol{\rho})$ can be considered a *bug*, in that it precludes a simplified yet valid calculation for the fourth-order moment of $h(\boldsymbol{\rho}', \boldsymbol{\rho})$. The next section will show how it can be turned into a *feature*, one that enables simple physical simulation of average intermodal cross talk.

4. PHYSICAL SIMULATOR FOR AVERAGE INTERMODAL CROSS TALK

A notional setup for a laboratory-scale physical simulator for measuring average intermodal cross talk is shown in Fig. 2. The concept here is as follows. The continuous-wave (cw) laser produces a beam in the fundamental

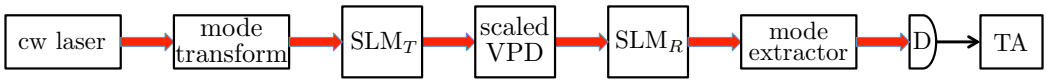

Figure 2: Notional setup for physical simulation of average intermodal cross talk. SLM$_T$ and SLM$_R$: transmitter-pupil and receiver-pupil spatial light modulators. Scaled VPD: scaled vacuum-propagation diffraction. D: detector. TA: time average.

TEM$_{00}$ Gaussian spatial mode. The mode-transform box converts that TEM$_{00}$ mode into a minified version of

the mth input mode of interest, to which spatial light modulator SLM_T applies a random-process phase tilt. The scaled VPD box in Fig. 2 bookends an $\tilde{L}$-m-long laboratory-propagation path with an appropriately chosen pair of lenses to mimic Fresnel diffraction over a much longer L m path. SLM_R then imposes another random-process phase tilt on the VPD box's output field. Finally, the mode-extractor box projects the component of its incident light that is in a minified version of the m'th output mode of interest on a photodetector. When the tilt statistics are chosen to realize a scaled version of the square-law structure function from Eq. (11), time averaging the fractional power transfer to the detector will, as we show below, yield $C_{m,m'}$ for Kolmogorov-spectrum turbulence whose Green's function mutual coherence is represented by Eq. (9) using the square-law approximation for $D(\boldsymbol{\rho}_1' - \boldsymbol{\rho}_2', \boldsymbol{\rho}_1 - \boldsymbol{\rho}_2)$. The details of the necessary scalings and tilt statistics are as follows.

- The output of the mode-transform box is a power-P_T field with complex envelope $\tilde{E}_0(\boldsymbol{\rho}) = \sqrt{P_T}\,\tilde{\Psi}_m^{(0)}(\boldsymbol{\rho})$, where
$$\tilde{\Psi}_m^{(0)}(\boldsymbol{\rho}) = (D_T/\tilde{D}_T)\Psi_m^{(0)}(\boldsymbol{\rho} D_T/\tilde{D}_T), \text{ for } \boldsymbol{\rho} \in \tilde{\mathcal{A}}_T \tag{19}$$
with $\tilde{\mathcal{A}}_T = \{\boldsymbol{\rho} : |\boldsymbol{\rho}| \le \tilde{D}_T/2\}$ for $\tilde{D}_T \ll D_T$.

- Spatial light modulator SLM_T, located in the $\tilde{\mathcal{A}}_T$ pupil, imposes a Gaussian random process phase-tilt $\exp(ik\tilde{\boldsymbol{\theta}}_0(t)\cdot\boldsymbol{\rho})$ on $\tilde{E}_0(\boldsymbol{\rho})$.

- The scaled-VPD box consists of a focal-length f lens in the $\tilde{\mathcal{A}}_T$ pupil, followed by $\tilde{L}$ m of diffraction to the $\tilde{\mathcal{A}}_R = \{\boldsymbol{\rho}' : |\boldsymbol{\rho}'| \le \tilde{D}_R/2\}$ pupil, where $\tilde{D}_R \ll D_R$, at which there is a focal-length f' lens. The values of f, $\tilde{L}$ and f' satisfy
$$\frac{1}{f} = \frac{1}{\tilde{L}} - \frac{(D_T/\tilde{D}_T)^2}{L}, \quad \tilde{L} = \frac{\tilde{D}_T\tilde{D}_R}{D_T D_R}\,L, \quad \frac{1}{f'} = \frac{1}{\tilde{L}} - \frac{(D_R/\tilde{D}_R)^2}{L}. \tag{20}$$

- Spatial light modulator SLM_R, located in the $\tilde{\mathcal{A}}_R$ pupil, imposes a Gaussian random process phase-tilt $\exp(ik\tilde{\boldsymbol{\theta}}_L(t)\cdot\boldsymbol{\rho}')$ on the field emerging from the scaled-VPD box, resulting in an output field with time-varying complex envelope $\tilde{E}_L(\boldsymbol{\rho}', t) = \sqrt{P_T}\,\tilde{\zeta}_m(\boldsymbol{\rho}', t)$.

- The mode-extractor box projects the
$$\tilde{\psi}_{m'}^{(0)}(\boldsymbol{\rho}') = (D_R/\tilde{D}_R)\psi_{m'}^{(0)}(\boldsymbol{\rho}' D_R/\tilde{D}_R), \text{ for } \boldsymbol{\rho}' \in \tilde{\mathcal{A}}_R \tag{21}$$
component of $\tilde{E}_L(\boldsymbol{\rho}', t)$ on the photodetector.

- The time-averaged fractional power transfer from $\tilde{E}_0(\boldsymbol{\rho})$ to the photodetector converges to the ensemble-average cross talk between the modes $\tilde{\Psi}_m^{(0)}(\boldsymbol{\rho})$ and $\tilde{\psi}_{m'}^{(0)}(\boldsymbol{\rho}')$, viz.,
$$\tilde{C}_{m,m'} \equiv \frac{\langle P_D(t)\rangle}{P_T} = \left\langle \left| \int_{\tilde{\mathcal{A}}_R} d\boldsymbol{\rho}'\, \tilde{\psi}_{m'}^{(0*)}(\boldsymbol{\rho}')\tilde{\zeta}_m(\boldsymbol{\rho}', t) \right|^2 \right\rangle, \tag{22}$$
where $P_D(t)$ is the power illuminating the detector at time t.

- The minified phase-tilts,
$$\boldsymbol{\theta}_0(t) = (\tilde{D}_T/D_T)\tilde{\boldsymbol{\theta}}_0(t) \quad \text{and} \quad \boldsymbol{\theta}_L(t) = (\tilde{D}_R/D_R)\tilde{\boldsymbol{\theta}}_L(t) \tag{23}$$
are a pair of zero-mean, jointly-Gaussian vector random processes whose covariance matrix at time lag $\tilde{L}/c$ is
$$\boldsymbol{\Lambda}_{4\mathrm{D}} \equiv \left\langle \begin{bmatrix} \theta_{0x}(t-\tilde{L}/c) \\ \theta_{Lx}(t) \\ \theta_{0y}(t-\tilde{L}/c) \\ \theta_{Ly(t)} \end{bmatrix} \begin{bmatrix} \theta_{0x}(t-\tilde{L}/c) & \theta_{Lx}(t) & \theta_{0y}(t-\tilde{L}/c) & \theta_{Ly}(t) \end{bmatrix} \right\rangle = \begin{bmatrix} \boldsymbol{\Lambda}_{2\mathrm{D}} & \mathbf{0} \\ \mathbf{0} & \boldsymbol{\Lambda}_{2\mathrm{D}} \end{bmatrix}, \tag{24}$$

where

$$\mathbf{\Lambda}_{2\mathrm{D}} = \frac{1}{k^2\rho_u^2}\begin{bmatrix} 8W/3 & (8/3 - W' - W)/2 \\ (8/3 - W' - W)/2 & 8W'/3 \end{bmatrix}, \tag{25}$$

with W, W', and ρ_u being the parameters of the square-law structure function from Eq. (11) for the C_n^2 profile to be simulated.

Having specified all the elements of the Fig. 2 simulator, we are ready to show that it works, i.e., that $C_{m,m'}$ from Eq. (8) for Kolmogorov turbulence whose mutual coherence function is evaluated using the square-law approximation from Eq. (11) satisfies

$$C_{m,m'} = \tilde{C}_{m,m'}. \tag{26}$$

The intuition behind this simulator is simple: if Gaussian statistics for phase tilts implies a Green's function mutual coherence characterized by a two-source, spherical-wave wave structure function of the form given in Eq. (11), then we have a simple, phase-tilt approach to simulating such a Green's function mutual coherence. The mathematics behind the simulator, i.e., the proof of Eq. (26), is as follows:

$$\tilde{C}_{m,m'} = \left\langle \left| \int_{\tilde{\mathcal{A}}_R} d\boldsymbol{\rho}'\, \tilde{\psi}_{m'}^{(0*)}(\boldsymbol{\rho}')\tilde{\zeta}_m(\boldsymbol{\rho}', t) \right|^2 \right\rangle \tag{27}$$

$$= \int_{\tilde{\mathcal{A}}_R} d\boldsymbol{\rho}_1' \int_{\tilde{\mathcal{A}}_R} d\boldsymbol{\rho}_2' \int_{\tilde{\mathcal{A}}_T} d\boldsymbol{\rho}_1 \int_{\tilde{\mathcal{A}}_T} d\boldsymbol{\rho}_2\, \tilde{\psi}_{m'}^{(0)}(\boldsymbol{\rho}_1')\tilde{\psi}_{m'}^{(0)*}(\boldsymbol{\rho}_2')\tilde{\Psi}_m^{(0)*}(\boldsymbol{\rho}_1)\tilde{\Psi}_m^{(0)}(\boldsymbol{\rho}_2)\langle \tilde{h}^*(\boldsymbol{\rho}_1', \boldsymbol{\rho}_1, t)\tilde{h}(\boldsymbol{\rho}_2', \boldsymbol{\rho}_2, t)\rangle, \tag{28}$$

where

$$\tilde{h}(\boldsymbol{\rho}', \boldsymbol{\rho}, t) = e^{ik\tilde{\boldsymbol{\theta}}_L(t)\cdot\boldsymbol{\rho}'} e^{-ik|\boldsymbol{\rho}'|^2/2f'} \frac{e^{ik(\tilde{L}+|\boldsymbol{\rho}'-\boldsymbol{\rho}|^2/2\tilde{L})}}{i\lambda\tilde{L}} e^{-ik|\boldsymbol{\rho}|^2/2f} e^{ik\tilde{\boldsymbol{\theta}}_0(t-\tilde{L}/c)\cdot\boldsymbol{\rho}} \tag{29}$$

is the concatenated Green's functions of SLM_T, the scaled VPD, and SLM_R. Substituting Eq. (29) into Eq. (28) and using the scaling relations given above leads to

$$\tilde{C}_{m,m'} = \int_{\mathcal{A}_R} d\boldsymbol{\rho}_1' \int_{\mathcal{A}_R} d\boldsymbol{\rho}_2' \int_{\mathcal{A}_T} d\boldsymbol{\rho}_1 \int_{\mathcal{A}_T} d\boldsymbol{\rho}_2\, \psi_{m'}^{(0)}(\boldsymbol{\rho}_1')\psi_{m'}^{(0)*}(\boldsymbol{\rho}_2')\Psi_m^{(0)*}(\boldsymbol{\rho}_1)\Psi_m^{(0)}(\boldsymbol{\rho}_2)$$
$$\times \frac{e^{-ik(|\boldsymbol{\rho}_1'-\boldsymbol{\rho}_1|^2-|\boldsymbol{\rho}_2'-\boldsymbol{\rho}_2|^2)/2L}}{(\lambda L)^2} \langle e^{-ik[\boldsymbol{\theta}_0(t-\tilde{L}/c)\cdot(\boldsymbol{\rho}_1-\boldsymbol{\rho}_2)+\boldsymbol{\theta}_L(t)\cdot(\boldsymbol{\rho}_1'-\boldsymbol{\rho}_2')]}\rangle. \tag{30}$$

Now, using the characteristic function for jointly-Gaussian random variables and our assumed tilt statistics, we find that

$$\tilde{C}_{m,m'} = \int_{\mathcal{A}_R} d\boldsymbol{\rho}_1' \int_{\mathcal{A}_R} d\boldsymbol{\rho}_2' \int_{\mathcal{A}_T} d\boldsymbol{\rho}_1 \int_{\mathcal{A}_T} d\boldsymbol{\rho}_2\, \psi_{m'}^{(0)}(\boldsymbol{\rho}_1')\psi_{m'}^{(0)*}(\boldsymbol{\rho}_2')\Psi_m^{(0)*}(\boldsymbol{\rho}_1)\Psi_m^{(0)}(\boldsymbol{\rho}_2)$$
$$\times \frac{e^{-ik(|\boldsymbol{\rho}_1'-\boldsymbol{\rho}_1|^2-|\boldsymbol{\rho}_2'-\boldsymbol{\rho}_2|^2)/2L}}{(\lambda L)^2} e^{-[|\boldsymbol{\rho}_1'-\boldsymbol{\rho}_2'|^2W'+(\boldsymbol{\rho}_1'-\boldsymbol{\rho}_2')\cdot(\boldsymbol{\rho}_1-\boldsymbol{\rho}_2)(8/3-W'-W)+|\boldsymbol{\rho}_1-\boldsymbol{\rho}_2|^2W]/2\rho_u^2}, \tag{31}$$

which is the desired result, i.e., it equals $C_{m,m'}$ for Kolmogorov-spectrum turbulence whose two-source, spherical-wave wave structure function is given by the square-law approximation.

5. CONCLUSIONS

Having demonstrated our principal objective—showing how a pair of phase tilts can be used to simulate average intermodal cross talk for Kolmogorov-spectrum turbulence within the square-law approximation for its two-source, spherical-wave wave structure function—let us conclude by briefly summarizing the strengths and weaknesses of this approach. Its core strengths are: (1) arbitrary mode sets and pupil geometries can be employed; (2) arbitrary non-uniform distributions of thick turbulence can be simulated; and (3) real, i.e., imperfect, modal multiplexers and demultiplexers can be used. Its major weaknesses are: (1) the square-law approximation does not perfectly capture the 5/3-law behavior of Kolmogorov-spectrum turbulence; (2) the absence of scintillation precludes this simulator's use to measure the error probabilities of modulated multiple spatial-mode communications, as was done in [6] for thin turbulence; and (3) only systems without adaptive optics can be simulated.

REFERENCES

[1] Guha, S., Dutton, Z. and Shapiro, J. H., "On quantum limit of optical communications: Concatenated codes and joint detection receivers," Digest 2011 IEEE Int. Symp. Inform. Theory, 274–278.

[2] Robinson, B. S., Kerman, A. J., Dauler, E. A., Barron, R. O., Caplan, D. O., Stevens, M. L., Carney, J. J., Hamilton, S. A., Yang, J. K. W. and Berggren, K. K., "781 Mbit/s photon-counting optical communications using a superconducting nanowire detector," Opt. Lett. 31(4), 444–446 (2006).

[3] Li, G., "Recent advances in coherent optical communication," Adv. Opt. Photon. 1(2), 279–307 (2009).

[4] Chandrasekaran, N. and Shapiro, J. H., "Photon information efficient communication through atmospheric turbulence—Part I: Channel model and propagation statistics," J. Lightw. Technol. 32(6), 1075–1087 (2014).

[5] Chandrasekaran, N., Shapiro, J. H. and Wang, L., "Photon information efficient communication through atmospheric turbulence—Part II: Bounds on ergodic classical and private capacities," J. Lightw. Technol. 32(6), 1088–1097 (2014).

[6] Ren, Y., Huang, H., Xie, G., Ahmed, N., Yan, Y., Erkmen, B. I., Chandrasekaran, N., Lavery, M. P. J., Steinhoff, N. K., Dolinar, S., Neifeld, M., Padgett, M. J., Boyd, R. W., Shapiro, J. H. and Willner, A. E., "Atmospheric turbulence effects on the performance of a free space optical link employing orbital angular momentum multiplexing," Opt. Lett. 38(20), 4062–4065 (2013).

[7] Ren, Y., Xie, G., Huang, H., Bao, C., Yan, Y., Ahmed, N., Lavery, M. P. J., Erkmen, B. I., Dolinar, S., Tur, M., Neifeld, M. A., Padgett, M. J., Boyd, R. W., Shapiro, J. H. and Willner, A. E., "Adaptive optics compensation of multiple orbital angular momentum beams propagating through emulated atmospheric turbulence," Opt. Lett. 39(10), 2845–2848 (2014).

[8] Strohbehn, J. W., ed., [Laser Beam Propagation in the Atmosphere], Springer-Verlag, Berlin, 171–222 (1978).

[9] Saleh, A. A. M., "An investigation of laser wave depolarization due to atmospheric transmission," IEEE J. Quantum Electron 3(11), 540–543 (1967).

[10] Shapiro, J. H., "Normal-mode approach to wave propagation in the turbulent atmosphere," Appl. Opt. 13(11), 2614–2619 (1974).

[11] Miller, D. A. B., "Establishing optimal wave communication channels automatically," J. Lightw. Technol. 31(24), 3987–3994 (2013).

[12] Slepian, D., "Prolate spheroidal wave functions, Fourier analysis and uncertainty—IV: Extensions to many dimensions; Generalized prolate spheroidal functions," Bell Syst. Tech. J. 43(6), 3009–3057 (1964).

[13] Lutomirski, R. F. and Yura, H. T., "Propagation of a finite optical beam in an inhomogeneous medium," Appl. Opt. 10(7), 1652–1658 (1971).

[14] Ishimaru, A., [Wave Propagation and Scattering in Random Media, vol. 2] Academic, New York, 412–422 (1978).

[15] Hardy, N. D. and Shapiro, J. H., "Computational ghost imaging versus imaging laser radar for three-dimensional imaging," Phys. Rev. A 87(2), 023820 (2013).

[16] Wandzura, S. M., "Meaning of quadratic structure functions," J. Opt. Soc. Am. 70(6), 745–747 (1980).